Program Digest, 2019 IEEE International Ultrasonics Symposium (IUS)
Glasgow, Scotland, October 6-9, 2019

Spatio-temporal compressed quantitative acoustic microscopy

J-H. Kim[1], J. Mamou[2], D. Kouamé[1], A. Achim[3], and A. Basarab[1]

[1]*IRIT UMR CNRS 5505, University of Toulouse, CNRS, INPT, UPS, UT1C, UT2J, France*
[2]*Frederic L. Lizzi Center for Biomedical Engineering, Riverside Research, New York, NY 10038, USA*
[3]*Visual Information Lab, SCEEM, University of Bristol, BS8 1UB, Bristol, UK*

***Abstract*—This study proposes an elegant spatio-temporal compressed sensing scheme to significantly reduce the amount of data required to form quantitative acoustic microscopy (QAM) images. QAM systems form two-dimensional acoustic parameter maps of thin section of soft tissues. QAM data collection consists in raster scanning a sample in 2D and digitizing backscattered RF signals at each scan location. Therefore, the raw QAM data is three-dimensional and when using this conventional data acquisition process, data sets can be large causing processing and storage limitations. Our previous work demonstrated that the amount of QAM data can be remarkably reduced either spatially or temporally by using compressive sampling (CS) or finite rate of innovation (FRI) approaches, respectively. These approaches take advantage of the properties of QAM data, *i.e.*, the sparsity of 2D maps and the parametric representation of RF signals. Therefore, in this study both approaches were combined into a single spatio-temporal solution. Results yielded a new data volume size of only 2.6% of the data originated by classical sampling techniques without significant deterioration of the 2D maps.**

***Index Terms*—quantitative acoustic microscopy, compressive sampling, finite rate of innovation, sparsity, parametric representation**

I. Introduction

Quantitative acoustic microscopy (QAM) is an ultrasound imaging modality using very high frequency ultrasound to form 2D maps of acoustic properties of soft tissues at microscopic scales [1], [2]. For our QAM system, thin *ex vivo* samples are affixed to a microscopy glass slides and are raster-scanned (spatial step size of 2 μm) using a 250 MHz transducer resulting in a 3D RF data cube. Each RF signal is processed to obtain, for each spatial location, acoustic parameters, *e.g.*, speed of sound (c). The scanning time is dependent on the sample size and can range from less than one minute to possibly tens of minutes. In order to prevent changes to the sensitive thin sectioned tissue during scanning, reducing scanning time is an important practical issue. In this regard, our previous studies were devoted to demonstrating: i) spatially under sampled measurements, following a spiral pattern combined with image reconstruction based on approximate message passing (AMP), allow decreasing the number of acquired RF signals by 40% without degrading the QAM image quality [3], ii) because QAM RF signals at a given location follow a parametric form with a limited number of degrees of freedom, each RF signal can be sampled (and adequately processed) at a much lower rate (162.5 MHz) than the Nyquist rate (800 MHz for our QAM system) [4]. The aim of this study is to combine AMP and FRI for QAM data to yield far more parsimonious data acquisition and to demonstrate that the combined approach significantly reduces QAM data acquisition time and QAM data size at no detriment to image quality.

The remainder of the paper is organized as follows. Section II covers the general theories of CS and FRI. Section III introduces the process of combining the spatial and temporal sparse encoding of QAM data, and subsequently Section IV details the decoding algorithm to yield 2D acoustic parametric maps. Section V compares the simulation results and the 2D map acquired by the traditional approach, and conclusions are presented in Section VI.

II. Theoretical background

A. Compressive sampling

Since its inception, the CS framework [5] has been used successfully in numerous applications where sparse or compressible signals (or images) can be exactly recovered from a small set of incoherent measurements (1) by solving a constrained optimization problem (2).

The CS measurement model is as follows

$$\mathbf{y} = \mathbf{\Phi}\mathbf{x} + \mathbf{n} \tag{1}$$

where $\mathbf{y} \in \mathbb{R}^M$ is the measurement vector, $\mathbf{x} \in \mathbb{R}^N$ is the signal or image to be reconstructed, $\mathbf{\Phi}$ is an $M \times N (M \ll N)$ measurement matrix and $\mathbf{n} \in \mathbb{R}^M$ is an additive white Gaussian noise. As a solver for this underdetermined problem, ℓ_1-norm minimization with relaxed constraints [6] is done as

$$\min_{\mathbf{x}\in\mathbb{R}^N} \|\mathbf{x}\|_1 \quad s.t. \quad \|\mathbf{y} - \mathbf{\Phi}\mathbf{x}\|_2 \leq \boldsymbol{\epsilon} \tag{2}$$

where $\boldsymbol{\epsilon}$ bounds the amount of noise in the measurements and is tuned to guarantee a perfect recovery with high probability as long as the measurement matrix satisfies the restricted isometry property (RIP) [7], and $M \geq C \cdot K \log(N/K)$ holds, where C is a positive constant and K is the number of non zero coefficients in the vector $\mathbf{x}$. AMP, that turns the reconstruction algorithm into an iterative denoising process, is an alternative to solving (2) for recovering an image from compressed

measurements [8]. In this work, an AMP algorithm, as briefly described in IV-B, is used for CS reconstruction [9], [10].

B. Finite Rate of Innovation

FRI signals, which are fully described by a limited number of parameters [11], can be recovered from a small set of samples acquired at the innovation rate ρ defined as

$$\rho = \lim_{\tau \to \infty} \frac{1}{\tau} C_x(-\frac{\tau}{2}, \frac{\tau}{2}) \tag{3}$$

where $C_x[t_a, t_b]$ represents a counting function that counts the number of parameters of $x(t)$ over the interval of time $[t_a, t_b]$. Interestingly, it has been shown that efficient recovery schemes are possible even in the case of non-bandlimited signals such as stream of Diracs, nonuniform splines and piecewise polynomials [11]. The key concept making the approach feasible is that the aforementioned class of signals can commonly be modeled as union of subspaces instead of a single linear vector space forcing an input signal to be bandlimited. A typical FRI signal is defined as

$$x(t) = \sum_{m \in Z} \sum_{l=0}^{L-1} a_l h(t - t_l - m\tau) \tag{4}$$

The signal above can be interpreted as living in a shift-invariant subspace spanned by a set of parameters, *i.e.*, time instances $\{t_l\}_{l=0}^{L-1}$ and amplitudes $\{a_l\}_{l=0}^{L-1}$ with a known basis $h(t)$ that is not necessarily band-limited. As such, given the basis function as a prior information, the novel sampling process carries out an uniform sampling at a dramatically reduced sampling rate, *i.e.*, the rate of innovation.

$$x_n = (x * g)(t)|_{t=nT} = \left\langle x(t), \varphi(\frac{t}{T} - n) \right\rangle \tag{5}$$

where $\varphi(t)$, as a scaled and time reversed version of $g(t)$, is called a sampling kernel and satisfies the generalized Strang-Fix conditions [12]. Retrieving $\{a_l, t_l\}_{l=0}^{L-1}$ from x_n is a standard problem in spectral analysis [13], and can be solved using conventional techniques such as the annihilating filter method [11].

III. Spatio-temporal sparse encoding

Hereafter, the two frameworks (*i.e.*, CS using AMP and FRI) are combined to achieve spatio-temporal undersampling of QAM data. The CS measurement in space uses a spiral scanning pattern because it is practical and could be easily implemented on typical QAM motor stages (instead of an impractical random-based measurement causing huge inefficiency). Fig. 1 illustrates the successive sampling process performed by CS and FRI frameworks. Firstly, the spiral pattern scanning is performed pointwise; only RF signals from these scan locations are retained, and are sampled using the FRI framework. As a result, the total amount of collected data was significantly reduced as depicted in the right cartoon in Fig. 1. As a final validation step, the 2D maps reconstructed from the CS data are quantitatively compared to the 2D maps obtained using the original fully sampled data.

A. Scanning pattern in spatial domain

CS measurement is basically established on an incoherent sampling, which proves to be generally satisfied by random linear combinations of the input data. However, there are many cases where it is inapplicable to build a random matrix approach in hardware due to practical issues such as high computational complexity or huge memory buffering. Inspired by previous CS literature [14], [15], in [3] we investigated the implementable sensing patterns for QAM systems and verified that the spiral pattern guarantees good recovery of QAM images.

B. Sampling kernel in time domain

QAM RF signals are made up of two primary reflections due to the water-tissue and tissue-glass interfaces, which can be modeled by the sum of two time-delayed, amplitude-decayed and frequency-dependent attenuated versions of a reference RF pulse as follow

$$x(t) = a_1 h(t - t_1) + a_2 h^*(t - t_2) \tag{6}$$

where the symbol $*$ stands for frequency-dependent attenuation. Since the information of the pulse shape $h(t)$ is commonly known as the characteristic of the transducer, (6) can be treated as an FRI signal defined in Section II-B. The sampling procedure used in this work is similar to the one proposed in [16]. The main idea is to sample uniformly the demodulated QAM signal using a finite support Sum of Sincs (SoS) sampling kernel and to relate these samples, through a linear model to the Fourier series coefficients $X[k]$. In the Fourier domain, the SoS sampling kernel (denoted by $\varphi(t)$ in the time domain) is given by

$$\Phi(\omega) = \frac{\tau}{\sqrt{2\pi}} \sum_{k \in Z} b_k sinc\left(\frac{\omega}{\frac{2\pi}{\tau}} - k\right), \tag{7}$$

where b_k is a smoothing window and has symmetric numbers of odd length for allowing a real valued analog filter. The discrete sequence of each RF signal is acquired by the following sampling process.

$$\begin{aligned} x[n] &= \langle x(t), \varphi(t - nT) \rangle \\ &= \sum_{k \in Z} X[k] e^{\frac{j2\pi knT}{\tau}} \Phi^*\Big[\frac{2\pi k}{\tau}\Big], \end{aligned} \tag{8}$$

where $(\cdot)^*$ symbolizes complex conjugation [4].

IV. Reconstruction of 2D acoustic maps

The reconstruction of 2D map begins by an auto-regressive (AR) parameter estimation [17] from the cubic data set, the result of which is equivalent to CS measurement in spatial domain as shown in Fig. 2(b). Therefore, the CS undersampling problem is solved by the AMP algorithm.

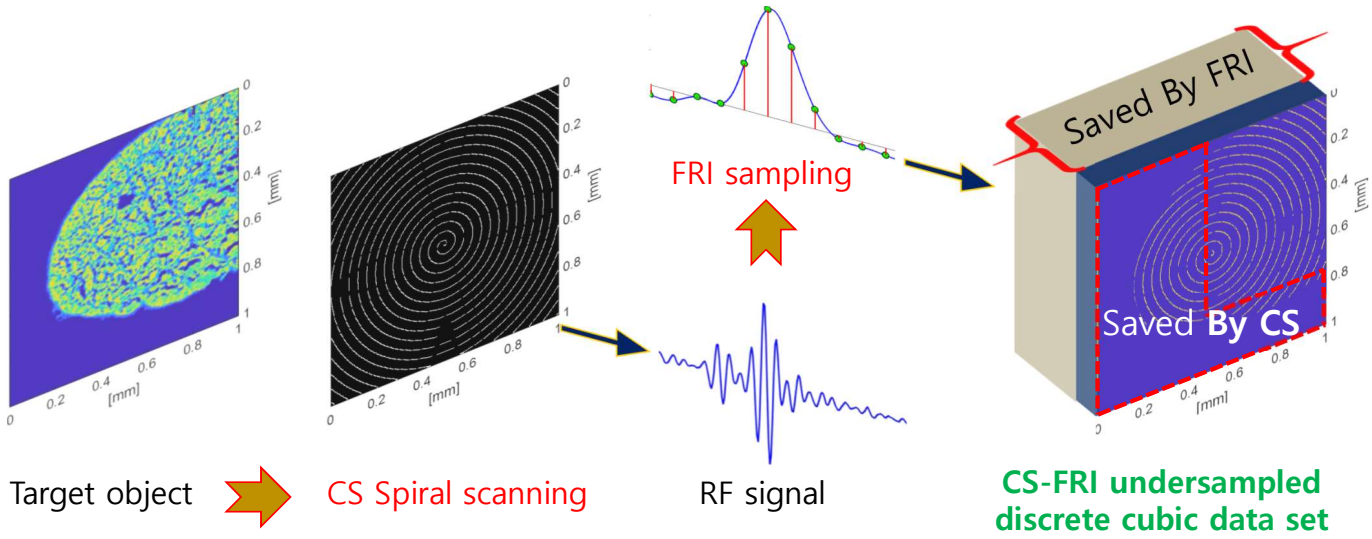

Fig. 1. The block diagram describes the undersampling process based on the spiral pattern and FRI sampling in spatial and temporal domain respectively. The right cartoon clearly demonstrates the space saved by the proposed sampling scheme.

A. Acoustic parameter estimation

From (8), using the observation $x[n]$ and the prior knowledge $\Phi[k]$, the Fourier coefficients $X[k]$ are identified. Subsequently, normalizing $X[k]$ with the Fourier coefficients of the known pulses, *i.e.*, $H[k]$, the following AR model is formulated as

$$N[k] = \sum_{l=1}^{n} a_l \{\exp[2\pi\Delta f(-\beta_l - j\Delta t_l)/\tau]\}^k = \sum_{l=1}^{n} a_l \lambda_l^k \tag{9}$$

Unknown parameters (λ_l and a_1) are determined by solving (9) (see [17] for details), and then the speed of sound (SOS) c is calculated by $c = c_w \frac{\text{imga}(\log\lambda_1)}{\text{imga}(\log\lambda_1)+\text{imga}(\log\lambda_2)}$, where c_w is the speed of sound in water.

B. Wavelet based Cauchy-AMP

The estimated SOS map is still incomplete due to undersampling carried out by the spiral scanning, and thus we accomplish the recovery process using AMP algorithm as follows

$$\begin{aligned} \boldsymbol{\theta}_{\mathbf{x}}^{t+1} &= \eta_t\left((\boldsymbol{\Phi}\,\boldsymbol{W}^{\ -1})^{\mathbf{T}}\mathbf{z}^t + \boldsymbol{\theta}_{\mathbf{x}}^t\right) \\ \mathbf{z}^t &= \mathbf{y} - (\boldsymbol{\Phi}\,\boldsymbol{W}^{\ -1})\boldsymbol{\theta}_{\mathbf{x}}^t \\ &\quad + \frac{1}{\delta}\mathbf{z}^{t-1}\left\langle \eta'_{t-1}\left((\boldsymbol{\Phi}\,W^{-1})^{\mathbf{T}}\mathbf{z}^{t-1} + \boldsymbol{\theta}_{\mathbf{x}}^{t-1}\right)\right\rangle \end{aligned} \tag{10}$$

where $\boldsymbol{\Phi}$ represents the spiral pattern, W is the wavelet transform employed as a sparsifying basis, and thus $\mathbf{x} = W^{-1}\boldsymbol{\theta}_{\mathbf{x}}$. η, which is a denoising function, is implemented as a Cauchy prior based Maximum A-Posteriori (MAP) estimator as [10]

$$\hat{w} = \eta(v) = \frac{v}{3} + s + t, \quad \hat{w}^{'} = \eta^{'}(v) = \frac{1}{3} + s^{'} + t^{'} \tag{11}$$

where the estimate $\hat{w}$ of clean wavelet coefficients w is acquired by denoising v corrupted by additive Gaussian noise, *i.e.*, $v = w + n$. On the other hand, s and t rely on v and σ_n^2.

V. Simulation Results

A 2D SOS map of a chicken tendon tissue (Fig. 2) was reconstructed using the proposed approach (*i.e.*, Fig. 1) from the compressed spiral cubic data set (40% less spatial data than classical raster scan and sampling rate of only 6.5% of the currently used rate as shown in the Table I). The spiral scanning pattern of Fig. 1 would allow to reduce the scan time by far more than 40% because of the continuous motion of the motors which is made possible through the smoothness of the spiral. Furthermore, significantly compressed data volume, *i.e.*, 2.6% compared to conventional method, could contribute to saving the required data storage space. In spite of the enormous decrease of data acquisitions, in the resulting images in Fig. 2 (g), no critical image degradation is perceived. The metrics in Table I support the visual evaluation.

VI. Conclusions

In this study, two approaches of CS and FRI sampling were combined, resulting into both shorter acquisition times and reduced amount of acquired data compared to the classical QAM sampling scheme. To confirm the preliminary results obtained in post-processing, hardware implementation on our QAM scanner will be carried out as a future work.

References

[1] D. Rohrbach, H. O. Lloyd, R. H. Silverman, R. Urs, and J. Mamou, "Acoustic-property maps of the cornea for improved high-frequency ultrasound corneal biometric accuracy," in *2015 IEEE International Ultrasonics Symposium (IUS)*, pp. 1–4, Oct 2015.

[2] D. Rohrbach, A. Jakob, H. O. Lloyd, S. H. Tretbar, R. H. Silverman, and J. Mamou, "A novel quantitative 500-mhz acoustic microscopy system for ophthalmologic tissues," *IEEE Transactions on Biomedical Engineering*, vol. 64, pp. 715–724, March 2017.

[3] J. Kim, J. Mamou, P. R. Hill, N. Canagarajah, D. Kouamé, A. Basarab, and A. Achim, "Approximate message passing reconstruction of quantitative acoustic microscopy images," *IEEE Transactions on Ultrasonics, Ferroelectrics, and Frequency Control*, vol. 65, pp. 327–338, March 2018.

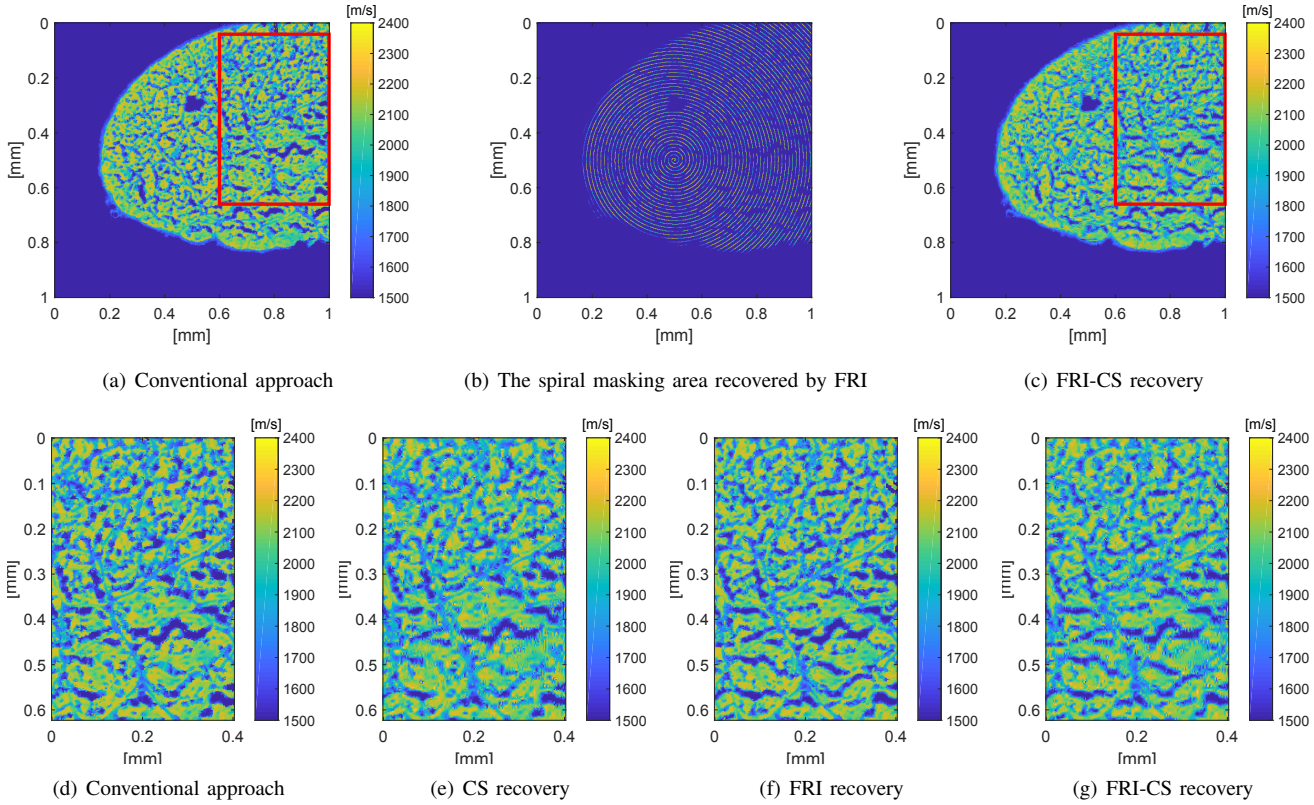

(a) Conventional approach (b) The spiral masking area recovered by FRI (c) FRI-CS recovery

(d) Conventional approach (e) CS recovery (f) FRI recovery (g) FRI-CS recovery

Fig. 2. The first row of the figure shows the recovery process of the SOS 2D map of a chicken tendon tissue. (a) is the original 2D map yielded by the conventional method, (b) is an intermediate result produced by estimating the SOS of the RF signals reflected from the only positions scanned by the spiral pattern, and finally (c) is the complete FRI-CS recovery result. The second row compares the SOS 2D map formed by the conventional approach (d) with the images (e-g) recovered from different methods.

Methods	Compressed Ratio			PSNR(dB)	NRMSE	SSIM
	Spatial	Temporal	Total volume (Spatial × Temporal)			
CS	40%	-	40%	26.31	0.0483	0.7166
FRI	-	6.5%	6.5%	24.19	0.0617	0.6741
FRI-CS	40%	6.5%	2.6%	23.38	0.0678	0.5511

TABLE I
Compressed ratio and resulting metrics according to different methods. The ratios of data reduction on this table correspond to 1004 scanning points on 40% of the spatial domain, and 13 samples on 6.5%the temporal axis.

[4] J. Kim, D. Kouamé, A. Basarab, J. Mamou, and A. Achim, "Reconstruction of quantitative acoustic microscopy images from rf signals sampled at innovation rate," in *2018 IEEE International Ultrasonics Symposium (IUS)*, pp. 1–4, IEEE, 2018.
[5] D. L. Donoho, "Compressed sensing," *Information Theory, IEEE Transactions on*, vol. 52, no. 4, pp. 1289–1306, 2006.
[6] E. J. Candès and M. B. Wakin, "An introduction to compressive sampling [a sensing/sampling paradigm that goes against the common knowledge in data acquisition]," *IEEE signal processing magazine*, vol. 25, no. 2, pp. 21–30, 2008.
[7] E. Candès and J. Romberg, "Sparsity and incoherence in compressive sampling," *Inverse problems*, vol. 23, no. 3, p. 969, 2007.
[8] D. L. Donoho, A. Maleki, and A. Montanari, "Message-passing algorithms for compressed sensing," *Proceedings of the National Academy of Sciences*, vol. 106, no. 45, pp. 18914–18919, 2009.
[9] J.-H. Kim, A. Basarab, P. R. Hill, D. R. Bull, D. Kouamé, and A. Achim, "Ultrasound image reconstruction from compressed measurements using approximate message passing," in *2016 24th European Signal Processing Conference (EUSIPCO)*, pp. 557–561, IEEE, 2016.
[10] P. R. Hill, J.-H. Kim, A. Basarab, D. Kouamé, D. R. Bull, and A. Achim, "Compressive imaging using approximate message passing and a cauchy prior in the wavelet domain," in *2016 IEEE International Conference on Image Processing (ICIP)*, pp. 2514–2518, IEEE, 2016.
[11] M. Vetterli, P. Marziliano, and T. Blu, "Sampling signals with finite rate of innovation," *IEEE Transactions on Signal Processing*, vol. 50, pp. 1417–1428, June 2002.
[12] I. Khalidov, T. Blu, and M. Unser, "Generalized l-spline wavelet bases," in *Wavelets XI*, vol. 5914, p. 59140F, International Society for Optics and Photonics, 2005.
[13] P. Stoica, R. L. Moses, *et al.*, "Spectral analysis of signals," 2005.
[14] T. Wan, N. Canagarajah, and A. Achim, "Compressive image fusion," in *2008 15th IEEE International Conference on Image Processing*, pp. 1308–1311, IEEE, 2008.
[15] C. Quinsac, A. Basarab, J.-M. Girault, and D. Kouamé, "Compressed sensing of ultrasound images: Sampling of spatial and frequency domains," in *2010 IEEE Workshop On Signal Processing Systems*, pp. 231–236, IEEE, 2010.
[16] R. Tur, Y. C. Eldar, and Z. Friedman, "Innovation rate sampling of pulse streams with application to ultrasound imaging," *Signal Processing, IEEE Transactions on*, vol. 59, no. 4, pp. 1827–1842, 2011.
[17] D. Rohrbach and J. Mamou, "Autoregressive signal processing applied to high-frequency acoustic microscopy of soft tissues," *IEEE Transactions on Ultrasonics, Ferroelectrics, and Frequency Control*, vol. 65, pp. 2054–2072, Nov 2018.